THE JOURNAL OF BIOLOGICAL CHEMISTRY
Vol. 275, No. 52, Issue of December 29, pp. 40938–40945, 2000

Printed in U.S.A.

Physical Characterization of the Procollagen Module of Human Thrombospondin 1 Expressed in Insect Cells*

Received for publication, August 3, 2000, and in revised form, September 20, 2000
Published, JBC Papers in Press, October 2, 2000, DOI 10.1074/jbc.M007022200

Tina M. Misenheimer‡, Kristin G. Huwiler, Douglas S. Annis, and Deane F. Mosher

From the Department of Medicine, University of Wisconsin, Madison, Wisconsin 53706

Thrombospondin 1 (TSP1) is a homotrimeric glycoprotein composed of 150-kDa subunits connected by disulfide bridges. The procollagen module of thrombospondin 1 has been implicated in antiangiogenic activity. Procollagen modules are found in a number of extracellular proteins and are identifiable by 10 cysteines with characteristic spacing. We expressed and studied the procollagen module (*C*) of human TSP1, both by itself and in the context of the adjoining oligomerization sequence (*o*) and N-terminal module (*N*). The coding sequences were introduced into baculoviruses along with an N-terminal signal sequence and C-terminal polyhistidine tag. Proteins were purified from conditioned medium of infected insect cells by nickel-chelate chromatography. *NoC* is a disulfide bonded trimer and cleaves readily at a site of preferential proteolysis to yield monomeric *N* and trimeric *oC*. These are known properties of full-length TSP1. Mass spectroscopy indicated that *C* is *N*-glycosylated, and all 10 cysteine residues of *C* are in disulfides. By equilibrium ultracentrifugation, *C* is a monomer in physiological salt solution. Circular dichroism, intrinsic fluorescence, and differential scanning calorimetry experiments suggest that the stability of *C* is determined by the disulfides. The two tryptophans of *C* are in a polar, exposed environment as assessed by iodide fluorescence quenching and solvent perturbation. The *oC* far UV circular dichroism spectrum could be modeled as the sum of *C* and a coiled-coil oligomerization domain. The results indicate that the recombinant *C* folds autonomously into its native structure, and trimerization of the modules in TSP1 does not perturb their structures.

Thrombospondin 1 (TSP1)[1] is a 450-kDa glycoprotein that is stored in the α-granules of platelets and is secreted by a number of cell types. Normally only present in very low quantities in plasma (1, 2), upon blood coagulation and activation of platelets, TSP1 is released into serum and is incorporated into fibrin clots (3, 4). TSP1 is composed of three identical 150-kDa monomers connected by disulfide bridges (5). Each monomer contains an N-terminal globular module (*N*), a central stalk region, and a globular C-terminal assemblage. The central stalk region is composed of the oligomerization sequence (*o*) that has the cysteines that form the interchain disulfide linkages, a procollagen module (*C*), three type 1 modules (properdin), and three type 2 modules (epidermal growth factor-like, EGF-like). The C-terminal assemblage is composed of 13 tandem aspartate-rich Ca^{2+} binding repeats and a globular C-terminal module. Functions of TSP1 include cell adhesion (6), inhibition of angiogenesis and endothelial cell proliferation (7), and activation of latent transforming growth factor-β (TGF-β) (8). The different modules mediate binding of TSP1 to cells, platelets, and numerous proteins such as collagen, fibronectin, heparan sulfate proteoglycan, laminin, fibrinogen, plasminogen, and histidine-rich glycoprotein (1, 2). Many of the interactions are mediated by *N*, which contains a heparin-binding site (9–11). *N* has also been found to mediate cellular internalization and degradation of TSP1 (12).

C has been implicated in the antiangiogenic activity of TSP1 (7), and its removal from TSP1 results in aberrant trimer formation (13). It is homologous to the cysteine-rich subdomain of the N-propeptide of procollagen α1(I), α1(II), α1(III), and α2(V) (14–16) (Fig. 1). The N-propeptide has been proposed to inhibit collagen synthesis (17, 18) and regulate the diameter of collagen fibrils by inhibiting the lateral growth during fibrillogenesis (19). The N-propeptide of type II procollagen has recently been shown to bind TGF-β1 and bone morphogenetic protein-2 (BMP-2) and has been proposed to play a role in the extracellular matrix deposition of BMPs in chondrogenic tissue (20).

Several other proteins contain modules homologous to *C*. The overall sequence identity in these modules is not high, but the cysteines are conserved (Fig. 1). The modules are sometimes called CR (for cysteine-rich). These proteins include such functionally diverse proteins as the large adhesive glycoprotein von Willebrand factor (vWF) that is required for platelet adhesion to damaged endothelium (21); the CCN family of growth-regulating immediate early response genes, including *cyr61*, *fisp-12*, *cef-10*, and connective tissue growth factor, which are expressed after induction by growth factors and certain oncogenes (22–24); *Xenopus* chordin (25) and *Drosophila* SOG (26), which are functionally homologous (27) and play crucial roles in dorsal-ventral patterning; and *Drosophila* SAS, which is required for larval development and has been suggested to

* This work was supported by funds from National Institutes of Health Grant HL54462 and utilized the University of Wisconsin-Madison Biophysics Instrumentation Facility, which is supported by National Science Foundation (NSF) Grant BIR-9512577, and a Bruker mass spectrometer, which was acquired using NSF Grant BIR-9520868. The costs of publication of this article were defrayed in part by the payment of page charges. This article must therefore be hereby marked "*advertisement*" in accordance with 18 U.S.C. Section 1734 solely to indicate this fact.

‡ To whom correspondence should be addressed: University of Wisconsin, 1300 University Ave., Madison, WI 53706. Tel.: 608-262-1375; Fax: 608-263-4969; E-mail: tmmisenh@facstaff.wisc.edu.

[1] The abbreviations used are: TSP1 and TSP2, thrombospondin 1 and 2, respectively; *C*, procollagen module of TSP1 without histidine tag; *C.coco*, procollagen module with histidine tag; *N*, N-terminal module of TSP1; *o*, oligomerization sequence of TSP1; *NoC*, trimeric N-terminal portion of TSP1 through the procollagen module including histidine tags; *oC*, trimeric procollagen module including the oligomerization sequence; DSC, differential scanning calorimetry; MALDI-MS, matrix-assisted laser desorption/ionization mass spectroscopy; DTT, dithiothreitol; GuHCl, guanidine hydrochloride; vWF, von Willebrand factor; TGF-β, transforming growth factor-β; BMP, bone morphogenetic protein; CR, cysteine-rich.

```
C, (hTSP1) ADPG*LRRPPL
           CYHNGVQYRNNEEWTVDS---CTE-CHCQNSVTI--------CKKVSCPIMP------------CSNAT--VPD-GECCPR--CWP*
                                                                                          LELVPR
hcollα1(I) CVQNGLRYHDRDVWKPEP---CQI-CVCDNGKVL--------CDDVICDETKN------------CPGAE--VPE-GECCPV--CPD
hvWFC1     CVHRSTIYPVGQFWEEG----CDV-CTCTDMEDAVMGLRVAQCSQKPCEDS--------------CRSGFTYVLHEGECCGR--CLP
mCYR61     CEYNSRIYQNGESFQPN----CKHQCTCIDGAVG--------CIPL-CPQELSLPNLG-------CPNPRL-VKVSGQCCEEWVCDE
xchordin2  CSFEGQLRAHGSRWAPDYDRKCSV-CSCQKRTVI--------CDPIVCPPLN------------CSQP---VHLPDQCCPV--CEE
dsas1      CLANNKSYKHGELMERD----CDERCTCNRGDWM--------CEPR-CRGLSYPRGSQRSMANPNCLEK---MLEEDECCRVMECSE

Pattern    C------y-----w-------C---C-C--------------C----C----------------C----------g-CC----C--
```

FIG. 1. **Expressed protein *C* and sequence alignment of procollagen modules.** The sequence of *C* begins on the *line above* the majority of the sequence and ends on the *line below* the sequence. The *asterisks* indicate the start and stop of residues encoded in human TSP1, with the remaining residues being the tails added from the vector. The conserved cysteines are in *boldface type*, the *first underlined sequence* is antiangiogenic as a peptide (7), and the *second underlined sequence* is a site of potential *N*-glycosylation. *h*, human; *m*, mouse; *x*, *Xenopus*; *d*, *Drosophila*; TSP1, (65); *coll α1(I)*, procollagen α1(I) (66); *vWFC1*, first of two homologous C modules in von Willebrand factor (21); CYR61 (23); *chordin2*, second of four homologous modules in chordin (25); *sas1*, first of four homologous modules in SAS (28).

function as an epidermal cell surface receptor (28). The procollagen module is repeated four times in chordin, SOG, and SAS; twice in vWF; and once in the other proteins. Spectroscopic characterization of proteolytically derived N-propeptide of sheep procollagen α1(I) showed that the protein is quite stable to denaturation and appears to contain aperiodic structural elements and β structure (29).

N has been proposed to be homologous to pentraxins as well as to a noncollagenous module (NC4) in α1(V), α1(IX), α1(XI), α1(XII), α1(XIV), and α1(XVI) collagens (30–32) that have predicted structures that contain a series of antiparallel β sheets. The x-ray structure of the pentraxin serum amyloid P component confirmed the presence of antiparallel β sheets arranged in two sheets in each subunit (33), as did the crystal structure of laminin α2 chain LG5 module, which is also related to *N* (34).

These observations raise the questions of whether *C* and *N* fold independently of the other modules and have structural properties of homologous modules. In order to answer these questions and to understand the structure/function of the modules, we have characterized recombinant *C* and *N* of human TSP1 using circular dichroism, fluorescence spectroscopy, differential scanning calorimetry, and analytical ultracentrifugation.

MATERIALS AND METHODS

Expression and Purification of C Using a Baculovirus Expression System and Nickel Chelate Chromatography—DNA encoding *C* was inserted into a baculovirus transfer vector (pAcGP67.coco) developed in our laboratory. Briefly, pAcGP67.coco is a modification of the baculovirus transfer vector pAcGP67A (Pharmingen) with the addition of a thrombin cleavage site (LVPRGS) and a six-histidine tag (His tag) immediately 3′ to the multiple cloning site. The cDNA encoding *C* (residues 294–356 of mature human TSP1) was polymerase chain reaction-amplified from a full-length cDNA clone of human TSP1 (generously donated by Dr. Vishva Dixit), inserted in the vector, and expressed in High Five insect cells (Invitrogen). The recombinant protein (*C.coco*) produced has the following sequence: ADPG ^{294}LRRPPL CYHNGVQYRN NEEWTVDSCT ECHCQNSVTI CKKVSCPIMP CSNATVPDGE CCPRCWP ^{356}LELVPR↓ GSAAGHHHHHH, where ↓ indicates the thrombin cleavage site. Leucine 294 was chosen as the start site for *C* because it is the N terminus of a 140-kDa fragment of TSP1 that was identified as an inhibitor of angiogenesis (35). Proline 356 was chosen as the end of the module based on the location of the intron-exon junction (36).

C.coco was expressed by infecting High Five cells in SF900II serum-free media with high titer virus (>10^8 pfu/ml) at MOI (multiplicity of infection) of 5–10. Conditioned medium was collected approximately 65 h postinfection, cells were spun down and removed, and 2 mM phenylmethylsulfonyl fluoride was added. The medium was then dialyzed into 50 mM sodium phosphate, 0.3 M NaCl, 7.5 mM imidazole, pH 8, and incubated with Ni^{2+}-nitrilotriacetic acid resin (Qiagen) overnight at 4 °C. The resin was washed with dialysis buffer, and *C.coco* was eluted with 50 mM sodium phosphate, 300 mM NaCl, 250 mM imidazole, pH 8.0. Overall yield was 20–25 mg of recombinant protein per liter of conditioned media.

The His tag was removed after dialysis of *C.coco* into 50 mM Tris, 150 mM NaCl, 2.5 mM $CaCl_2$, pH 8.5, by digestion with 2 units of biotinylated thrombin (Novagen)/mg of protein overnight at room temperature. Thrombin was removed using streptavidin-agarose (Novagen). Undigested protein was removed by purification with Ni^{2+}-nitrilotriacetic acid, as described above, and 1 mM Pevabloc (Roche Molecular Biochemicals) was added. Protein concentration was determined using absorbance at 280 nm and a calculated extinction coefficient of 14,605 M^{-1} cm^{-1} (37). Amino acid analysis was used to confirm the extinction coefficient (data not shown). *C* (procollagen module without the His tag) was concentrated using Centriplus 3 concentrators (Amicon) and purified further using an Amersham Pharmacia Biotech S-100 gel filtration column equilibrated in 25 mM sodium phosphate, 300 mM NaCl, pH 7, buffer.

Expression and Purification of the N-terminal Portion of Thrombospondin 1 (NoC) Using a Baculovirus Expression System and Nickel Chelate Chromatography—The N-terminal end of TSP1 through the end of *C* (residues 1–374) was expressed in High Five insect cells using the same expression system as above. The expressed protein was purified using Ni^{2+}-nitrilotriacetic acid resin in a similar manner as above for *C.coco*, except the medium was incubated with the resin without prior dialysis. Imidazole (5 mM) was added to the medium during incubation with the resin, and the resin was washed with 10 mM Tris, 150 mM NaCl, 0.3 mM $CaCl_2$, pH 7.4 (TBSC), containing 20 mM imidazole prior to elution of *NoC* with TBSC containing 300 mM imidazole. The eluted *NoC* was dialyzed into 50 mM Tris, 300 mM NaCl, 2.5 mM $CaCl_2$, pH 8.5, prior to storage at −70 °C. Overall yield was 4–5 mg of recombinant protein per liter of conditioned medium.

Trypsin Digestion of NoC—*N* was cleaved off of *NoC* by digesting with trypsin (1:500, w/w) at 37 °C for 30–60 min. The digest was purified using a heparin column (Amersham Pharmacia Biotech) equilibrated in TBSC. The flow-through contained the trimer composed of the oligomerization sequence through the procollagen modules (*oC*). *N* was eluted using 10 mM Tris, 0.55 M NaCl, 0.3 mM $CaCl_2$, pH 7.4. Digestions were followed using SDS-PAGE, and gels were stained using Gel-Code Blue (Pierce). Protein concentrations were determined using calculated extinction coefficients of 70,005 M^{-1} cm^{-1} for *NoC*, 48,660 M^{-1} cm^{-1} for *oC* and 7115 M^{-1} cm^{-1} for *N* (37).

Molecular Weight Determination—The mass was determined by matrix-assisted laser desorption/ionization mass spectroscopy (MALDI-MS) using a Bruker REFLEX II (Billerica, MA) equipped with delayed extraction, reflectron, and a 337-nm laser. The matrix was a saturated solution of α-cyano-4-hydroxycinnaminic acid (Sigma). The calibrants were insulin and trypsinogen (Sigma). The acceleration voltage, positive ion mode, was 25 kV. Protein was prepared prior to analysis by extensive dialysis into 5% acetic acid. Molecular weight was determined via equilibrium analytical ultracentrifugation using a Beckman analytical ultracentrifuge at 27,000, 36,000, and 40,000 rpm at 4 °C. Protein was 0.1–0.35 mg/ml in 25 mM sodium phosphate, 0.3 M NaCl, pH 7, buffer.

Circular Dichroism—CD studies were performed on an Aviv circular dichroism spectrometer, model 62A DS. Far UV measurements were taken in a 0.1-cm path length cuvette using protein dialyzed into 25 mM sodium phosphate, pH 7.4, while near UV measurements were taken in a 1-cm path length cuvette using protein dialyzed into 50 mM sodium phosphate, 0.3 M NaCl, pH 7, buffer. Time constants were either 5 or 10 s. Three scans were averaged for each measurement and base line-subtracted. The resulting spectra were converted to mean residue weight ellipticity and smoothed using Aviv's Igor Pro software. Thermal stability of *C* was examined by monitoring the ellipticity at 228 nm every 5 °C as temperature was raised from 25 to 95 °C at 50 °C/min. The SOPM program was used for secondary structure prediction (38), while the K2D program (39, 40) was used for deconvolution of the CD

spectrum. The probability of a coiled-coil in the oligomerization sequence was examined by sequence analysis using the Paircoil (41) and COILS (38, 42) programs.

Intrinsic Fluorescence—Steady state emission spectra were obtained at 25 °C using an SLM-8000C fluorimeter. Excitation and emission slit widths were 2 and 4 nm, respectively. Tryptophan emission was observed using excitation at 295 nm. Buffer was 10 mM Tris-HCl, 150 mM NaCl, 0.3 mM $CaCl_2$, pH 7.4 (TBSC) with or without 10 mM dithiothreitol (DTT) or 6 M ultrapure guanidine hydrochloride (GuHCl) (ICN Biomedicals). Three scans were averaged for each measurement and base line-subtracted. Corrections due to inner filter effects were not incorporated, since the absorbance values did not exceed 0.01.

Fluorescence Quenching—In order to determine the average accessibility of emissive tryptophans in *C* and *N*, fluorescence quenching experiments with acrylamide and KI were performed at 25 °C. Protein in 25 mM sodium phosphate, pH 7.4, was quenched in the presence of increasing amounts of acrylamide (0–100 mM) or KI (0–100 mM). The KI stock solution also contained 0.1 mM potassium thiosulfate in order to prevent formation of I_3^-. The fluorescence measurements were performed as described above, as continuous emission spectra between 300 and 400 nm with excitation at 295 nm. Tryptophan fluorescence intensities were obtained for each experiment by integrating the fluorescence spectra. The fluorescence quenching data were analyzed according to the Stern-Volmer equation which is $F_o/F = 1 + \mathrm{Ksv}\,[Q]$, where F_o and F are the integrated fluorescence intensities in the absence or presence of quenchers, respectively, K_{sv} is the collisional Stern-Volmer constant, and [Q] is the quencher concentration (43, 44). The plot of F_o/F *versus* [Q] is linear if the population of emitting fluorophores is homogeneous.

Solvent Perturbation—The solvent accessibility of the tryptophan residues in *C* was examined by measuring the differential absorbance spectra in the presence and absence of 20% glycerol in 25 mM sodium phosphate, pH 7.4, buffer. Measurements were made using tandem cuvettes in a Hitachi U-2000 spectrophotometer. Four scans were averaged for each measurement. The change in the extinction coefficient at 292 nm was used to estimate the exposure of the tryptophan residues as described by Herskovits (45). An equimolar mixture of the *N*-acetyl ethyl esters of tryptophan and tyrosine was used as the model compound.

Calorimetry—Differential scanning calorimetry (DSC) was done using a Microcal differential scanning calorimeter with *C* at 1.5 mg/ml in 50 mM sodium phosphate, 0.3 M NaCl, pH 7. The scans were from 15 to 95 °C at a rate of 60 °C/h.

Migration Assay—Endothelial cell migration was measured in a 48-well chemotaxis chamber (Nucleopore) with cells and mediators in Dulbecco's modified Eagle's medium plus 0.2% fatty acid-free bovine serum albumin as described by Tolsma *et al.* (7). Polyvinylpyrrolidone-free polycarbonate membranes with 5-μm pores (Whatman) were coated with collagen I (Upstate Biotechnologies, Inc., Lake Placid, NY) before use. Calf pulmonary artery endothelial cells (VEC Technologies) or fetal bovine heart endothelial cells (American Tissue Culture Collection) were plated at 25,000 cells/well and allowed to adhere to the lower surface of a membrane in an inverted chemotaxis chamber for 2 h at 37 °C. The chamber was reinverted, and test samples were added to the top wells and incubated for 4 h at 37 °C to allow migration. Dulbecco's modified Eagle's medium with 0.2% fatty acid-free bovine serum albumin was used as a negative control, and 1 μM sphingosine 1-phosphate (Alexis Corp.) was used as the stimulant (46).

Other Procedures—N-terminal sequencing was generously provided by Dr. Johan Stenflo (University of Lund, Sweden). The protein was run on SDS-PAGE and transferred to polyvinylidene difluoride membrane, where it was stained with Amido Black prior to sequencing. Amino acid analysis for determining the extinction coefficient was done at the Biotechnology Center of the University of Wisconsin. The presence of glycosylation of *C* was tested using a digoxigenin glycan detection kit (Roche Molecular Biochemicals) as directed by the manufacturer, and by treating *C.coco*-infected SF9 cells with 5 μg/ml tunicamycin. *C* with or without 6 M guanidine hydrochloride was reduced with DTT in 0.25 M Tris, 2 mM EDTA, pH 8.5, prior to alkylation with iodoacetic acid (47, 48).

RESULTS

General Characterization of C—*C* was expressed and purified as described under "Materials and Methods." N-terminal sequencing showed *C* began with ADPGLRRPPL, indicating that the signal sequence was cleaved. The expected mass was 8204.5 Da (Table I). On SDS-PAGE under reducing conditions, the protein migrated as an approximately 10,000-Da protein (Fig. 2*A*). Under nonreducing conditions, it migrated as a smear, most likely due to binding of SDS at substoichiometric amounts due to the high disulfide bond content. MALDI-MS yielded peaks with masses of 9090, 9239, 9406, and 9575 Da (Fig. 2*B*). *C* has one consensus sequence for *N*-linked glycosylation (NAT) at residues 354–356. The mass difference observed via MALDI-MS is explained by glycosylation of *C* with (*N*-acetylglucosamine)$_2$(mannose)$_3$ (mass 911 Da) along with an additional sugar or two (each sugar adds an additional 150–180 Da depending on the type). The presence of glycosylation was verified using a digoxigenin glycan kit. Treatment of infected cells with tunicamycin, an inhibitor of *N*-glycosylation, greatly reduced protein secretion and resulted in protein of the expected unmodified mass by SDS-PAGE, further indicating that *C* is glycosylated (data not shown).

TABLE I
Molecular weight of C

The masses of the four peaks observed using MALDI-MS presented are the average of four determinations. Error was <0.1%.

Mass expected	SDS-PAGE	Equilibrium ultracentrifugation	MALDI-MS
Da	*Da*		*Da*
8204.5	10,000	9483 ± 30	9091, 9244, 9408, 9584

Equilibrium analytical ultracentrifugation of *C* at concentrations of 0.1–0.35 mg/ml was done in order to determine its molecular weight and aggregation state in physiologic salt solution. The molecular weight was determined to be 9483 ± 30 (Table I). This agreed with the MALDI-MS mass and indicates that *C* is monomeric.

In order to determine the disulfide bond content of *C*, the protein was denatured, reduced, and alkylated. The masses of the iodoacetic acid-treated native protein, denatured protein, and denatured/reduced protein were determined by MALDI-MS and compared (Table II). A mass shift due to alkylation was only detected after reductive exposure of all cysteine residues.

Expression and Trypsin Digestion of the N-terminal Portion of TSP1 (NoC)—The N-terminal portion of TSP1, *NoC*, was also expressed in insect cells using recombinant baculovirus and purified using nickel chelate chromatography as described under "Materials and Methods." The yield of *NoC* was only 4–5 mg/liter of conditioned medium, compared with the 20–25 mg/liter yield for *C*. *NoC*, unlike *C*, had a tendency to aggregate. Consequently, the salt concentration was kept higher in the buffer, and the protein needed to be filtered free of aggregates prior to use.

As described earlier, *NoC* is expected to be a trimeric protein containing three *N* modules and three *C* modules connected into a trimer via the disulfide linkages in the oligomerization sequence, *o*, of TSP1. Nonreduced *NoC* migrated as two bands (124 and 96 kDa) on an SDS-PAGE (Fig. 3*A*). The 96-kDa band can be attributed to some of the purified trimeric protein (*NoC*) missing one of the three *N* modules due to the lability of the sequence between *N* and *o* to proteolytic cleavage (49). This is supported by the observation that after 2 min of trypsin digestion, a band at 67 kDa appeared, presumably due to *NoC* missing two *N* modules, as well as a band at 41 kDa due to *oC* and one at 28 kDa due to *N*. After 15 min, only monomeric *N* (28 kDa) and trimeric *oC* (41 kDa) were apparent (Fig. 3).

N and *oC* were purified from the trypsin digest of *NoC* using heparin-agarose as described under "Materials and Methods." The purified *N* and *oC* are shown on Gel-Code Blue stained SDS-polyacrylamide gel to be free of undigested *NoC* (Fig. 3). The purified *oC* was subjected to N-terminal sequencing and found to have two N-termini, TKDLQAI and DLQAI, indicating that trypsin cleaved after lysine 250 and lysine 252. The puri-

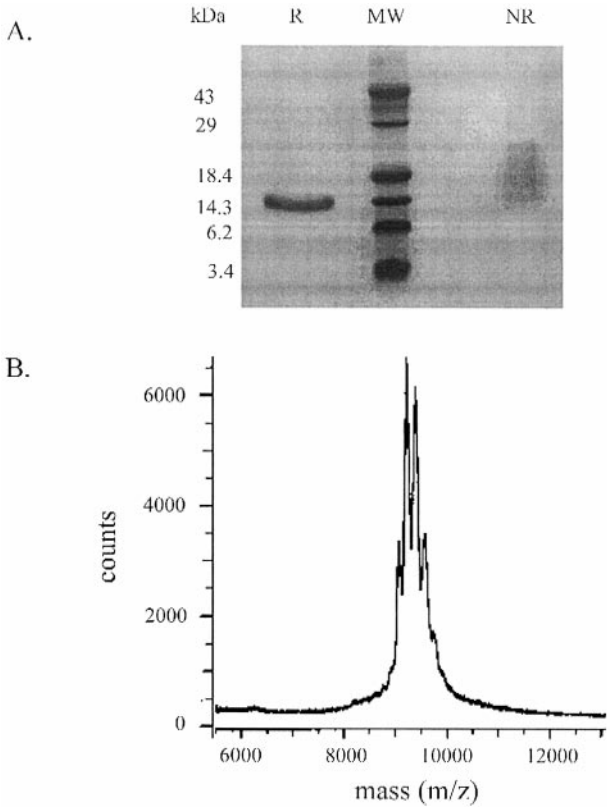

FIG. 2. *A*, SDS-PAGE of an 18% polyacrylamide gel stained with Gel-Code Blue of reduced (*R*) and nonreduced (*NR*) *C*. *B*, MALDI-MS spectrum of *C*. *MW*, molecular weight.

TABLE II
Determination of disulfide bond content of C

C with or without 6 M GuHCl was reduced with DTT in 0.25 M Tris, 2 mM EDTA, pH 8.5, buffer prior to alkylation with iodoacetic acid (IA). The reaction was quenched and prepared for MALDI-MS by dialysis into 5% acetic acid. The table lists the change in the mass of the second MALDI-MS peak (Fig. 2*B*, 9244 Da) upon treatment and relates the change to number of carboxymethyl (CM) groups.

Treatment	Mass (peak 2)	Mass change from native	Mass change/ Mass CM
	Da	*Da*	
GuHCl/IA	9240	−4.4	<0.1
DTT/IA	9832	588	10.1
GuHCl/DTT/IA	9817	573	9.9

fied *oC* was unable to bind to the nickel resin, indicating that trypsin cleavage of *NoC* also removed the histidine tag.

Circular Dichroism Studies—In order to compare the structures of *C*, *oC*, *N*, and *NoC*, their far UV circular dichroism spectra were measured (Fig. 4). The far UV CD spectrum of *C* showed a positive band with a maximum at 228 nm and a negative band with a minimum at 202 nm. The far UV CD spectrum of *oC* was quite different from that of *C*. A large positive band at 190 nm and negative bands at 208 and 222 nm were observed in *oC*, while the positive band at 228 nm was not present. The expected contribution of *C* to the far UV CD spectrum of *oC* is 58.7% based on relative masses. When the contribution of *C* is subtracted from the observed *oC* spectrum, the resulting spectrum resembles that expected for a coiled-coil with minima at 208 and 220 nm (Fig. 4*A*).

The spectra of *N* and *NoC* were consistent with the presence of a β sheet (50). Both had a positive band around 190 nm. *N* had a broad negative band at 214 nm, while *NoC* had two negative bands at 210 and 220 nm. The spectra resembled the

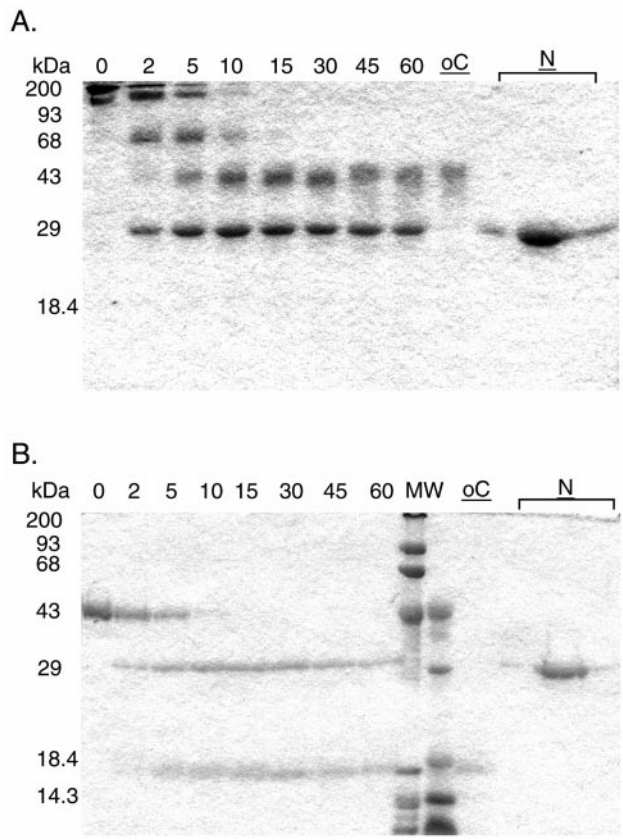

FIG. 3. **Time course of trypsin digestion of *NoC* followed by SDS-PAGE of a 14% polyacrylamide gel under nonreducing (*A*) and reducing conditions (*B*) as described under "Materials and Methods."** *Lanes 1–8*, 0-, 2-, 5-, 10-, 15-, 30-, 45-, and 60-min time points. *Lanes* to the *right* show molecular weight markers (*MW*) and heparin-agarose-purified *oC* and *N*, respectively.

spectra for the pentraxins human C-reactive protein (51) and PTX3 (52). The expected contribution of *N* and *oC* to the far UV CD spectrum of *NoC* based on relative masses would be 32.3% *oC* and 64.9% *N*. The observed *NoC* spectrum matched the expected spectrum given the error in determination of protein concentration (Fig. 4*B*), indicating that the global fold of *N* is not altered significantly by trimer formation.

Heat Denaturation of C Studied Using CD and DSC—The stability of *C* was examined using CD and DSC studies. Upon heating, the far UV CD signal at 228 nm decreased gradually without any sign of cooperative conformation changes (Fig. 5). Only one broad peak was observed during DSC with an approximate melting point of 85 °C (Fig. 5), and the melting was not found to be reversible (data not shown). The far UV CD spectrum of *C* at 90 °C lacked the peak at 228 nm and looked like the far UV CD spectrum of *C* reduced with 2 mM DTT (Fig. 6). Reduction of *C* with 2 mM DTT unfolded *C* within 5 min at room temperature. In the near UV, a small positive peak was observed at 255 nm, most likely due to the disulfides (50), while a shallow negative trough was apparent at 290 nm due to the tryptophan residues. Upon heating, the signals gradually disappeared (Fig. 7).

Fluorescence Studies—The modules were examined in their native and denatured conformations using fluorescence spectroscopy. The fluorescence emission spectrum of *C* (which contains two tryptophan residues), upon excitation at 295 nm, revealed a wavelength of maximum fluorescence (λ_{max}) of 351 nm, indicating that the tryptophan residues are in a polar environment in the native protein. The addition of 6 M GuHCl shifted this slightly to 352 nm (Fig. 8*A*). The further addition of

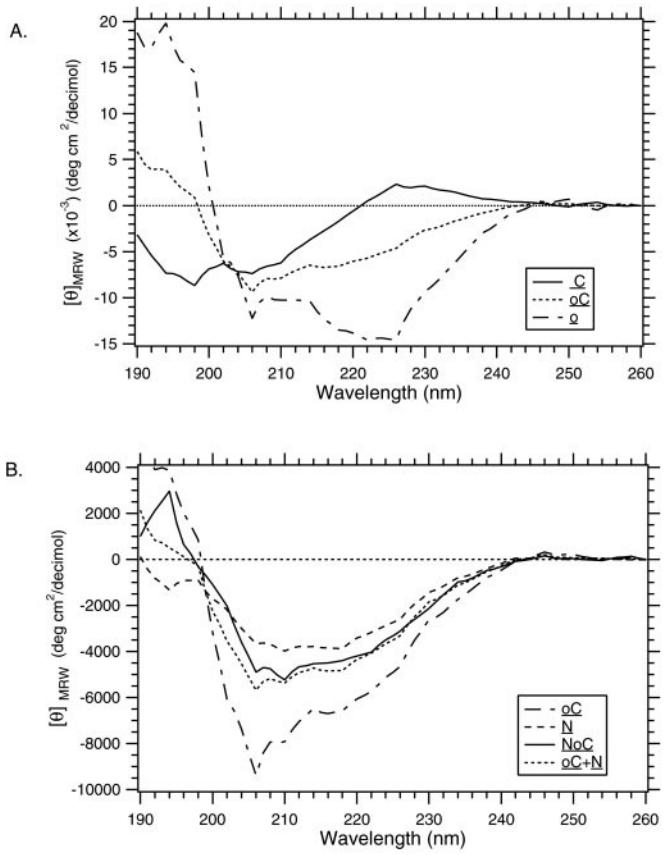

FIG. 4. **Far UV circular dichroism spectra of *C* and *oC*, in 25 mM sodium phosphate, pH 7.4, and *o* spectrum predicted after subtraction of 58.7% *C* (relative mass) from the observed *oC* spectrum (*A*) and *N*, *NoC*, and *oC*, in 25 mM sodium phosphate, pH 7.4, and *NoC* spectrum predicted from the addition of the observed *N* and *oC* spectra using the relative masses of 64.9% *N* and 35.1% *oC* (*B*).** Data were collected at 25 °C and are expressed as mean residue weight molar ellipticity ($[\theta]_{MRW}$). There are 73, 345, 48, 1131, and 251 residues in *C*, *oC*, *o*, *NoC*, and *N*, respectively.

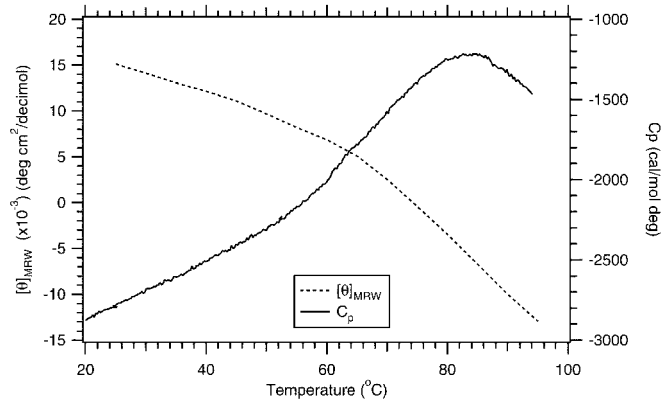

FIG. 5. **Temperature-induced unfolding of *C* was monitored using CD to observe the change in mean residue weight molar ellipticity ($[\theta]_{MRW}$) at 228 nm of 105 μM *C* in 25 mM sodium phosphate, pH 7, buffer and differential scanning calorimetry to measure the heat capacity (C_p) of 158 μM *C* in 50 mM sodium phosphate, 300 mM NaCl, pH 7, buffer**.

10 mM DTT to 6 M guanidine hydrochloride shifted the spectrum to a λ_{max} of 353 nm. The addition of 10 mM DTT alone had little effect. The same results were observed after excitation at 280 nm (data not shown).

The fluorescence emission spectra of *oC* (which contains six tryptophan residues per trimer) was similar to that of *C* in regard to shape and position of emission maximum, but the

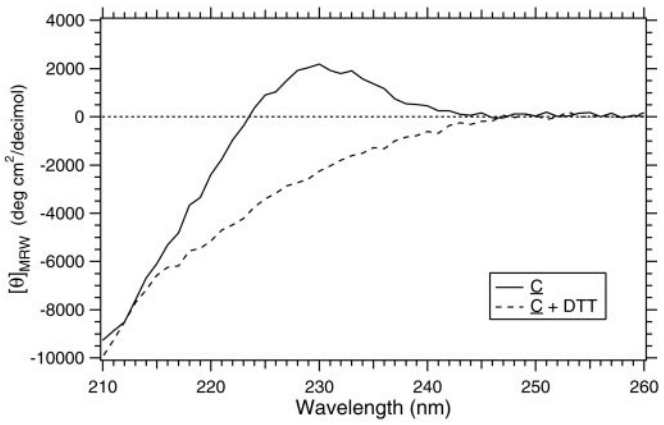

FIG. 6. **Reduction of *C* was monitored using far UV CD.** The CD spectrum of *C* in 25 mM sodium phosphate, pH 7.4, with or without 2 mM DTT was collected at 25 °C. The reduced spectrum was measured 5 min after the addition of DTT. Data are expressed as mean residue weight molar ellipticity ($[\theta]_{MRW}$).

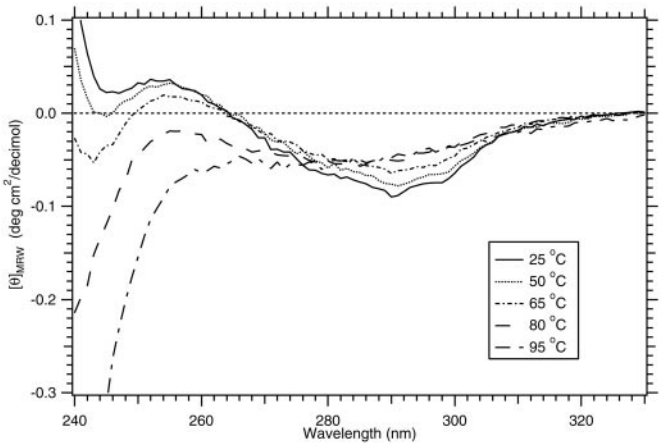

FIG. 7. **Temperature-induced unfolding of *C*.** Temperature-induced unfolding of *C* was monitored by observing changes in the near UV CD spectra of 47 μM *C* in 50 mM sodium phosphate, 300 mM NaCl, pH 7, buffer at 25, 50, 65, 80, and 95 °C. Data are expressed as mean residue weight molar ellipticity ($[\theta]_{MRW}$).

fluorescence intensity of the *oC* spectrum was much lower (Fig. 8*B*). Under native conditions, the λ_{max} of *oC* was 350 nm. Denaturation shifted the λ_{max} to 353 nm.

The fluorescence emission spectrum of *N* (which contains one tryptophan per module) indicated that its tryptophan residue was in a nonpolar environment in the native protein. The λ_{max} was 334 nm in TBSC with or without DTT *versus* 352 nm in TBSC plus 6 M GuHCl and DTT (Fig. 8*C*). The relative fluorescence intensity of *N* was considerably higher than that of *C* on an equimolar basis. The fluorescence emission spectrum of *NoC* (which contains nine tryptophans per trimer, only three of which are in *N*) most closely resembled the spectrum of *N*. The λ_{max} was 335 nm and was shifted to 352 nm upon the addition of 6 M GuHCl with or without DTT (Fig. 8*D*). DTT alone shifted the λ_{max} to 339 nm.

Fluorescence Quenching Studies—In order to examine the environment of the tryptophans of *C* and *N*, the ability of KI and acrylamide to quench the fluorescence emission spectra was examined. Both acrylamide and KI quench the fluorescence intensity of *N* and *C*. The Stern-Volmer plots were linear, but the magnitude of the quenching constants differed (Table III). Analysis of the quenching data for *N* yielded quenching constants (K_{sv}) of 13.9 and 9.8 M^{-1} for KI and acrylamide, respectively, indicating that the tryptophan residues in *N* are solvent-accessible. Analysis of the quenching data for *C* yielded

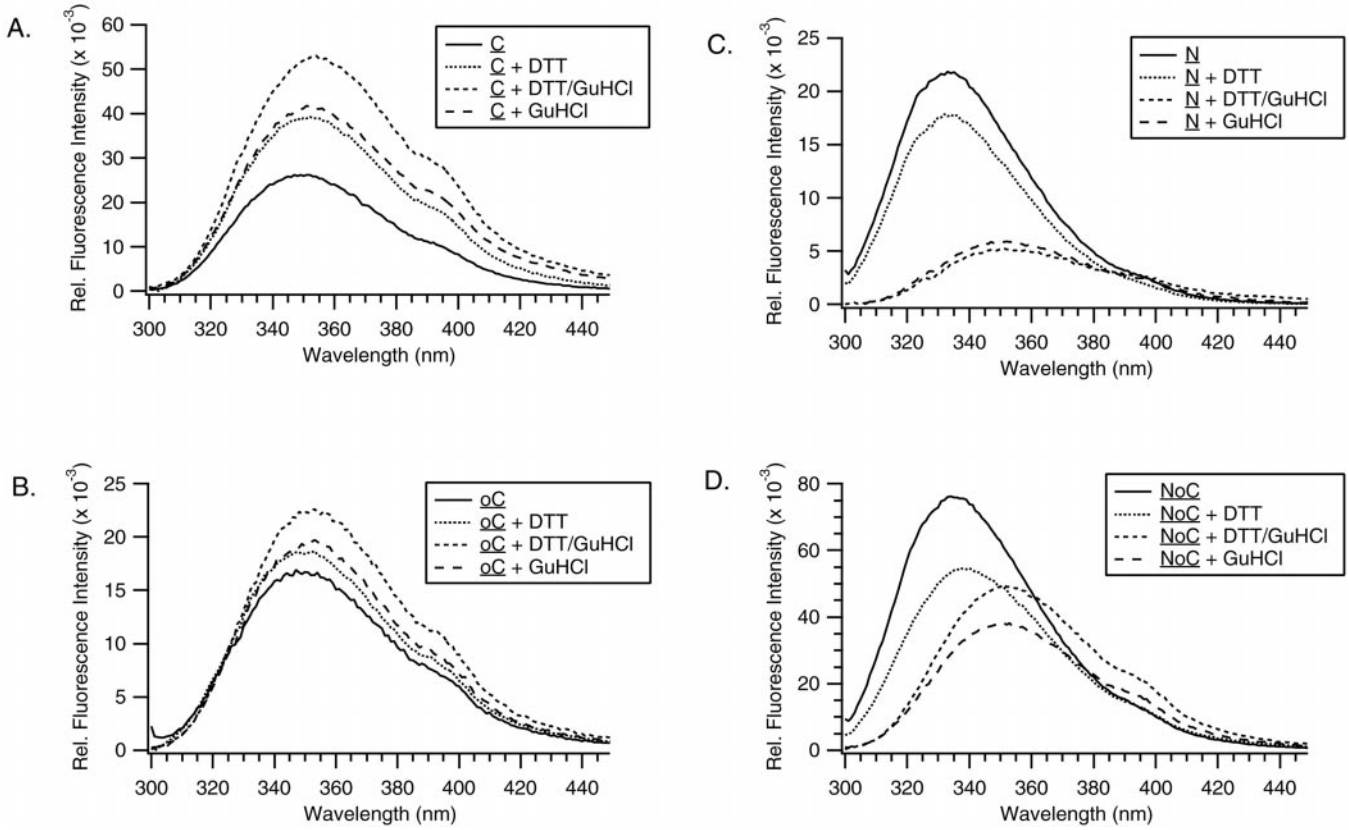

FIG. 8. **Fluorescence emission spectra of 1.5 μM *C* (*A*), 0.5 μM *oC* (*B*), 0.5 μM *N* (*C*), and 0.5 μM *NoC* (*D*) were measured at 25 °C in TBSC; TBSC plus 10 mM DTT, TBSC plus 10 mM DTT, 6 M GuHCl; and TBSC + 6 M GuHCl with excitation at 295 nm.**

TABLE III
Fluorescence properties of C and N

Emission peak maximums (λ_{max}) were determined from the steady state fluorescence spectra after excitation at 295 nm. The dynamic quenching constants (K_{sv}) for iodide and acrylamide were calculated using the Stern-Volmer equation (see "Materials and Methods").

Protein	λ_{max}	Iodide, K_{sv}	Acrylamide, K_{sv}
	nm	M^{-1}	M^{-1}
C	351	3.9	10.3
N	334	13.9	9.8

quenching constants of 3.9 and 10.3 M^{-1} for KI and acrylamide, respectively, indicating that the tryptophan residues in *C* are solvent-accessible but probably in a negatively charged or neutral environment.

Solvent Perturbation Studies—Fluorescence studies indicated that the tryptophans of *C* were in a polar environment and accessible to quenching by KI and acrylamide. To further characterize the exposure of the tryptophans, the solvent accessibility of the tryptophans was examined by measuring the differential absorbance spectra in the presence and absence of 20% glycerol (Fig. 9). The positive peak at 292 nm is characteristic for perturbation of tryptophans by a nondenaturing solvent additive like glycerol. Comparison of the magnitude of this change to that obtained for model tryptophan and tyrosine compounds indicated that both tryptophans are solvent-accessible (45).

Migration Assays—The ability of the recombinant *C* to inhibit endothelial cell migration was examined as described under "Materials and Methods." In six different experiments, *C* consistently did not inhibit fetal bovine heart endothelial cell or calf pulmonary artery endothelial cell migration, but TSP1 frequently did not inhibit migration either. In the most informative experiment, fetal bovine heart endothelial cell migration

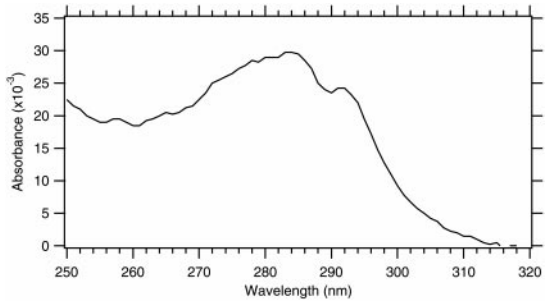

FIG. 9. **Solvent perturbation difference spectrum of *C*.** *C* (28 μM) in 25 mM sodium phosphate, pH 7.4, buffer was perturbed with 20% glycerol using tandem cuvettes.

was inhibited by 8% with 150 nM *C*, while platelet TSP1 at 0.4 nM inhibited 40% of the migration toward sphingosine 1-phosphate. Therefore, we have no evidence that recombinant *C* will attenuate migration of endothelial cells as has been reported (7, 53).

DISCUSSION

Baculovirus expression and purification of *C* from human TSP1 resulted in large quantities of purified protein that by several criteria are folded and processed correctly. Recombinant *C* was glycosylated and contained 10 cysteines, all in disulfide bonds. The far UV CD spectrum had a positive band at 228 nm and a negative band at 202 nm with no evidence of α-helix (Fig. 4). Secondary structure prediction of *C* based on amino acid sequence indicates that the protein is 67% random coil, 20% extended strand, and 12% β-turn, while deconvolution of the observed CD spectrum using K2D (39, 40) predicts 51% β-sheet, 42% random coil, and 7% α-helix. Prediction of α-helix and β-sheet content through deconvolution of our CD data can only give a general idea of secondary structure, however, be-

cause we were unable to collect data below 190 nm due to interference by solvent. Engel *et al*. observed a remarkably similar far UV CD spectrum for the homologous cysteine-rich N-propeptide of sheep type 1 procollagen purified after proteolysis of native protein and concluded that the N-propeptide had no α-helix but rather a tightly packed aperiodic structure with β structure similar to β-trypsin (29).

The conformation of *C* was stable to temperature. CD and DSC both showed that the protein unfolds gradually without cooperativity (Fig. 5). DSC results indicated that the melting point is about 85 °C. Such stability was also observed for the N-propeptide of sheep type 1 procollagen (29). Since *C* has five disulfides, the role the disulfides play in maintaining the structure was examined using CD and intrinsic fluorescence. Upon reduction with DTT, the intrinsic fluorescence intensity of *C* increased (Fig. 8), suggesting that the protein is partially unfolded in the absence of disulfide linkages. A similar change occurred upon the addition of GuHCl. The increase in fluorescence intensity upon denaturation indicates the tryptophans were quenched in the native conformation, possibly due to nearby polar residues. Far UV CD revealed that upon reduction with DTT, *C* unfolds rapidly at room temperature (Fig. 6). Therefore, the stability of *C* appears to be predominantly due to the five disulfide linkages. The gradual loss of structure upon heating is probably due to local unfolding of the secondary structural elements that link the disulfides.

The procollagen module has been proposed to aid in multimerization of TSP1, TSP2, the procollagens, and vWF (14). The trimeric *Drosophila* protein peroxidasin has also been found to contain a procollagen module near its proposed oligomerization site (54). TSP1 lacking *C* was primarily expressed as dimers and monomers by mouse NIH 3T3 cells (13). But TSP1 truncated before *C* consisted largely of intact trimers when expressed in COS cells or insect cells (11), and dimerization of vWF has been found to involve only the C-terminal 151 amino acids and not the procollagen homology modules C1 and C2 (55). Our equilibrium analytical ultracentrifugation experiment showed that the recombinant *C* is a monomeric protein that does not have a tendency to aggregate. This evidence supports the view that *C* does not cause oligomer formation, although it may stabilize oligomer formation of the proteins containing it.

TSP1 has been proposed to form a trimeric coiled-coil structure that is stabilized by interchain disulfides (11). The oligomerization region of TSP5, which is pentameric, has been crystallized and shown to be a pentameric coiled-coil (56). Coiled-coils are readily predicted on the basis of a heptad repeat, $(a\text{-}b\text{-}c\text{-}d\text{-}e\text{-}f\text{-}g)_n$, which contains hydrophobic residues at positions *a* and *d* (57). Sequence analysis of the oligomerization sequence of human TSP1 using the Paircoil (41) and COILS (38, 42) programs predicts a coiled-coil structure for residues 271–293 within the oligomerization sequence. This sequence has at least four heptad repeats with predominantly leucine and valine at positions *a* and *d*. Leucine and valine in these positions have been found to favor dimeric and trimeric coiled-coils (57). The far UV CD spectrum of the *oC* trimer was quite different from that of the monomeric *C* (Fig. 4*A*). The positive band at 228 nm was not present in the spectrum of the *oC* trimer; instead, a double minimum at 208 and 222 nm and a maximum at 190 nm were observed. These bands are indicative of α-helix (50). When the contribution of *C* is subtracted from the observed *oC* spectrum, the resulting spectrum resembles that expected for a coiled-coil (Fig. 4*A*).

Both monomeric *C* and trimeric *oC* have 350 nm as a wavelength of maximum fluorescence (Fig. 8), indicating that under native conditions the tryptophans in *C* are in a polar environment in both the monomeric and the trimeric protein. Fluorescence intensity, however, was quenched by 32% in the trimeric protein. This decreased fluorescence intensity can be explained by energy transfer effects due to proximity of the three modules in *oC*. The efficiency of energy transfer, *E*, equals $R_o^6/(R_o^6 + r^6)$, where R_o is the Förster distance at which efficiency of transfer is 50%, and *r* is the distance between donor and acceptor molecules (58). The critical distances range from 2 to 5 nm. Assuming the individual *C* module is an ellipsoid 3–4 nm long (the length of the similarly sized properdin module) (59), the maximum distance between the distal ends of two ellipsoids in the *oC* trimer would be 5–7 nm apart. Depending on where the two tryptophans are located in the ellipsoids, tryptophans in adjacent ellipsoids may be only 1.5–2 nm apart. Energy transfer between the tryptophans, therefore, would be expected to occur and could easily account for the decrease in quantum yield of tryptophan fluorescence in *oC*. Equilibrium analytical ultracentrifugation showed that the recombinant *C* is a monomeric protein that does not have a tendency to aggregate. Therefore, it is proximity forced by the trimeric coiled-coil, rather than any self-interaction, that probably brings the *C* modules together without change in the structure of the individual modules.

TSP1, a TSP1 fragment beginning with *C*, and a peptide with the sequence NGVQYRN that was derived from *C* have been found to be antiangiogenic (7). Since one tryptophan is near the NGVQYRN sequence (Fig. 1), the properties of the tryptophan residue give us an indication of the environment of the NGVQYRN sequence. Solvent perturbation, fluorescence quenching, and the wavelength of maximum fluorescence indicate that the two tryptophan residues of *C* are in a polar, solvent-accessible environment. Thus, the NGVQYRN sequence probably is also exposed in the native protein and solvent-accessible. Recently, contrary to the initial report that the sequence NGVQYRN defines a minimal sequence within the TSP1 procollagen module capable of inhibiting corneal neovascularization (7), two other groups have not been able to show inhibitory activity for the peptide in either the CAM or corneal assay (60, 61). Recombinant TSP1 procollagen module made in *Escherichia coli* also failed to inhibit vascularization in the CAM assay (61). These reports indicate that the procollagen module probably does not inhibit neovascularization *in vivo* and is accord with our unsuccessful attempts to demonstrate antimigratory activity.

The procollagen module, frequently termed the CR module (for cysteine-rich), is found in many proteins including TSP1, TSP2, fibrillar procollagens, vWF, Cyr61, and chordin. Since the structure of *C* and the N-propeptide of type 1 collagen appear to be similar, the homologous CR modules in other proteins probably also have a similar structure. The sequences of the CR modules are quite different, but the cysteine residues are identical (Fig. 1). Both our data and the analysis of sequence conservation indicate that the global fold of the CR module is primarily dependent on the conserved cysteines and five disulfide linkages. The functions of these proteins are diverse. The CR module has been proposed to have a conserved function for binding TGF-β family members (26). The relationships among CR-containing proteins and the TGF-β family members are complex. The cysteine-rich N-propeptide of type II procollagen has been found to bind TGF-β and BMP-2 (20), and TSP1 is also a TGF-β-binding protein (62). Procollagen expression is linked to expression of TGF-β, and TGF-β induces procollagen gene expression (26) and also expression of CCN family members (24). Dorsal-ventral patterning in vertebrate and *Drosophila* embryos involves a conserved system of extracellular proteins including BMP or its *Drosophila* homolog,

DPP; a BMP/DPP antagonist, chordin/SOG; a secreted metalloproteinase, xolloid/tolloid, that cleaves chordin/SOG; and twisted gastrulation (TSG), a BMP/DPP agonist. Chordin/SOG has four CR modules. The CR1 and CR3 modules of chordin have dorsalizing activity in *Xenopus* embryo assays and bind BMP-4 (63). TSG contains an N-terminal region proposed to be homologous to the CR modules of chordin, although this region of TSG has 14 instead of 10 cysteines. This cysteine-rich region of TSG also binds BMPs (64). The determinations of the functions of the CR modules of these proteins, TSP1, TSP2, and other proteins have been hampered by the lack of pure protein. Our studies describing a facile method to express and purify an individual CR module and characterization of its structure at low resolution should serve as a foundation for rigorous structure/function analyses of CR modules in general.

REFERENCES

1. Mosher, D. F. (1990) *Annu. Rev. Med.* **41,** 85–97
2. Frazier, W. A. (1991) *Curr. Opin. Cell Biol.* **3,** 792–799
3. Bale, M. D., and Mosher, D. F. (1986) *J. Biol. Chem.* **261,** 862–868
4. Murphy-Ullrich, J. E., and Mosher, D. F. (1985) *Blood* **66,** 1098–1104
5. Bornstein, P. (1992) *FASEB J.* **6,** 3290–3299
6. Lawler, J., Weinstein, R., and Hynes, R. O. (1988) *J. Cell Biol.* **107,** 2351–2361
7. Tolsma, S. S., Volpert, O. V., Good, D. J., Frazier, W. A., Polverini, P. J., and Bouck, N. (1993) *J. Cell Biol.* **122,** 497–511
8. Crawford, S. E., Stellmach, V., Murphy-Ullrich, J. E., Ribeiro, S. M. F., Lawler, J., Hynes, R., Boivin, G. P., and Bouck, N. (1998) *Cell* **93,** 1159–1170
9. Lahav, J. (1993) *Biochim. Biophys. Acta* 1–14
10. Bornstein, P. (1995) *J. Cell Biol.* **130,** 503–506
11. Sottile, J., Selegue, J., and Mosher, D. F. (1991) *Biochemistry* **30,** 6556–6562
12. Mikhailenko, I., Krylov, D., Argraves, K. M., Roberts, D. D., Liau, G., and Strickland, D. K. (1997) *J. Biol. Chem.* **272,** 6784–6791
13. Lawler, J., Ferro, P., and Duquette, M. (1992) *Biochemistry* **31,** 1173–1180
14. Hunt, L. T., and Barker, W. C. (1987) *Biochem. Biophys. Res. Commun.* **144,** 876–882
15. Woodbury, D., Benson-Chanda, V., and Ramirez, F. (1989) *J. Biol. Chem.* **264,** 2735–2738
16. Ryan, M. C., and Sandell, L. J. (1990) *J. Biol. Chem.* **265,** 10334–10339
17. Fouser, L., Sage, E. H., Clark, J., and Bornstein, P. (1991) *Proc. Natl. Acad. Sci. U. S. A.* **88,** 10158–10162
18. Wu, C. H., Donovan, C. B., and Wu, G. Y. (1986) *J. Biol. Chem.* **261,** 10482–10484
19. Chapman, J. A. (1989) *Biopolymers* **28,** 1367–1382
20. Zhu, Y., Oganesian, A., Keene, D. R., and Sandell, L. J. (1999) *J. Cell Biol.* **144,** 1069–1080
21. Mancuso, D. J., Tuley, E. A., Westfield, L. A., Worrall, N. K., Shelton-Inloes, B. V., Sorace, J. M., Alevy, Y. G., and Sadler, J. E. (1989) *J. Biol. Chem.* **264,** 19514–19527
22. Bradham, D. M., Igarashi, A., Potter, R. L., and Grotendorst, G. R. (1991) *J. Cell Biol.* **114,** 1285–1294
23. Ryseck, R.-P., MacDonald-Bravo, H., Mattei, M.-G., and Bravo, R. (1991) *Cell Growth Differ.* **2,** 225–233
24. Bork, P. (1993) *FEBS Lett.* **327,** 125–130
25. Sasai, Y., Lu, B., Steinbeisser, H., Geissert, D., Gont, L. K., and DeRobertis, E. M. (1994) *Cell* **79,** 779–790
26. Francois, V., Soloway, M., O'Neill, J. W., Emergy, J., and Bier, E. (1994) *Genes Dev.* **8,** 2602–2616
27. Holley, S. A., Jackson, P. D., Sasai, Y., Lu, B., DeRobertis, E. M., Hoffmann, F. M., and Ferguson, E. L. (1995) *Nature* **376,** 249–336
28. Schonbaum, C. P., Organ, E. L., Qu, S., and Cavener, D. R. (1992) *Dev. Biol.* **151,** 431–445
29. Engel, J., Bruckner, P., Becker, U., Timpl, R., and Rutschmann, B. (1977) *Biochemistry* **16,** 4026–4033
30. Beckmann, G., Hanke, J., Bork, P., and Reich, J. G. (1998) *J. Mol. Biol.* **275,** 725–730
31. Moradi-Ameli, M., Deleage, G., Geourjon, C., and Van Der Rest, M. (1994) *Matrix Biol.* **14,** 233–239
32. Bork, P. (1992) *FEBS Lett.* **307,** 49–54
33. Emsley, J., White, H. E., O'Hara, B. P., Oliva, G., Srinivasan, N., Tickle, I. J., Blundell, T. L., Pepys, M. B., and Wood, S. P. (1994) *Nature* **367,** 338–345
34. Hohenester, E., Tisi, D., Talts, J. F., and Timpl, R. (1999) *Mol. Cell* **4,** 783–792
35. Good, D. J., Polverini, P. J., Rastinejad, F., Le Beau, M. M., Lemons, R. S., Frazier, W. A., and Bouck, N. P. (1990) *Proc. Natl. Acad. Sci. U. S. A.* **87,** 6624–6628
36. Wolf, F. W., Eddy, R. L., Shows, T. B., and Dixit, V. M. (1990) *Genomics* **6,** 685–691
37. Schmid, F. X. (1997) in *Protein Structure: A Practical Approach* (Creighton, T. E., ed) pp. 261–298, Oxford University Press, New York
38. Lupas, A., Van Dyke, M., and Stock, J. (1991) *Science* **252,** 1162–1164
39. Andrade, M. A., Chacon, P., Merelo, J. J., and Moran, F. (1993) *Protein Eng.* **6,** 383–390
40. Merelo, J. J., Andrade, M. A., Prieto, A., and Moran, F. (1994) *Neurocomputing* **6,** 443–454
41. Berger, B., Wilson, D. B., Wolf, E., Tonchev, T., Milla, M., and Kim, P. S. (1995) *Proc. Natl. Acad. Sci. U. S. A.* **92,** 8259–8263
42. Lupas, A. (1996) *Methods Enzymol.* **266,** 513–525
43. Eftink, M. R., and Ghiron, C. A. (1981) *Anal. Biochem.* **114,** 199–227
44. Lehrer, S. S., and Leavis, P. C. (1978) *Methods Enzymol.* **49,** 222–236
45. Herskovits, T. T. (1967) *Methods Enzymol.* **11,** 748–775
46. Panetti, T. S., Nowlen, J. K., and Mosher, D. F. (2000) *Arterioscler. Thromb. Vasc. Biol.* **20,** 1013–1019
47. Wada, Y. (1996) in *Protein and Peptide Analysis by Mass Spectrometry* (Chapman, J. R., ed) pp. 101–113, Humana Press, Inc., Totowa, NJ
48. Rademaker, G. J., and Thomas-Oates, J. (1996) in *Methods in Molecular Biology* (Chapman, J. R., ed) pp. 231–241, Humana Press Inc., Totowa, NJ
49. Lawler, J. W., and Slayter, H. S. (1981) *Thromb. Res.* **22,** 267–279
50. Woody, R. W. (1995) *Methods Enzymol.* **246,** 34–71
51. Miyazawa, K., and Inoue, K. (1990) *J. Immunol.* **145,** 650–654
52. Bottazzi, B., Vouret-Craviari, V., Bastone, A., De Gioia, L., Matteucci, C., Peri, G., Spreafico, F., Pausa, M., D'Ettorre, C., Gianazza, E., Tagliabue, A., Salmona, M., Tedesco, F., Introna, M., and Mantovani, A. (1997) *J. Biol. Chem.* **272,** 32817–32823
53. Dawson, D. W., Pearce, S. F. A., Zhong, R., Silverstein, R. L., Frazier, W. A., and Bouck, N. P. (1997) *J. Cell Biol.* **138,** 707–717
54. Nelson, R. E., Fessler, L. I., Takagi, Y., Blumberg, B., Keene, D. R., Olson, P. F., Parker, C. G., and Fessler, J. H. (1994) *EMBO J.* **13,** 3438–3447
55. Voorberg, J., Fontijn, R., Calafat, J., Janssen, H., van Mourik, J. A., and Pannekoek, H. (1991) *J. Cell Biol.* **113,** 195–205
56. Malashkevich, V. N., Kammerer, R. A., Efimov, V. P., Schulthess, T., and Engel, J. (1996) *Science* **274,** 761–765
57. Woolfson, D. N., and Alber, T. (1995) *Protein Sci.* **4,** 1596–1607
58. Lakowicz, J. R. (1983) *Principles of Fluorescence Spectroscopy*, pp. 305–339, Plenum Press, New York
59. Smith, K. F., Nolan, K. F., Reid, K. B. M., and Perkins, S. J. (1991) *Biochemistry* **30,** 8000–8008
60. Kanda, S., Shono, T., Tomasini-Johansson, B., Klint, P., and Saito, Y. (1999) *Exp. Cell Res.* **252,** 262–272
61. Iruela-Arispe, M. L., Lombardo, M., Krutzsch, H. C., Lawler, J., and Roberts, D. D. (1999) *Circulation* **100,** 1423–1431
62. Murphy-Ullrich, J. E., Schultz-Cherry, S., and Höök, M. (1992) *Mol. Biol. Cell* **3,** 181–188
63. Larrain, J., Bachiller, D., Lu, B., Agius, E., Piccolo, S., and DeRobertis, E. M. (2000) *Development* **127,** 821–830
64. Oelgeschlager, M., Larrain, J., Geissert, D., and DeRobertis, E. M. (2000) *Nature* **405,** 757–763
65. Lawler, J., and Hynes, R. O. (1986) *J. Cell Biol.* **103,** 1635–1648
66. Tromp, G., Kuivaniemi, H., Stacey, A., Shikata, H., Baldwin, C. T., Jaenisch, R., and Prockop, D. J. (1988) *Biochem. J.* **253,** 919–922